Research Article | Vol. 25, No. 21 | 16 Oct 2017 | OPTICS EXPRESS 26067

Optics EXPRESS

Indistinguishable heralded single photon generation via relative temporal multiplexing of two sources

X. ZHANG,[1,2] Y. H. LEE,[3,4] B. A. BELL,[1,2] P. H. W. LEONG,[2,3] T. RUDOLPH,[5] B. J. EGGLETON,[1,2,*] AND C. XIONG[1,2]

[1]*Centre for Ultrahigh bandwidth Devices for Optical Systems (CUDOS), Institute of Photonics and Optical Science (IPOS), School of Physics, University of Sydney, NSW 2006, Australia*
[2]*The Australian Institute for Nanoscale Science and Technology (AINST), University of Sydney, NSW 2006, Australia*
[3]*School of Electrical and Information Engineering, University of Sydney, NSW 2006, Australia*
[4]*VeCAD Research Laboratory, Faculty of Electrical Engineering, Universiti Teknologi Malaysia, 81310 Skudai, Johor, Malaysia*
[5]*Department of Physics, Imperial College London, Prince Consort Road, London SW7 2AZ, UK*
**egg@physics.usyd.edu.au*

Abstract: Generating *N* single photons simultaneously is a formidable challenge due to the lack of deterministic single photon sources. Recent work [New J. Phys. **19**, 063013 (2017)] has proposed a relative multiplexing scheme that can enhance the *N* single photons probability with a minimum of active switching resources. We experimentally demonstrate relative temporal multiplexing on two photon sources with a 90% additional enhancement over the standard temporal multiplexing scheme demonstrated previously. 88 ± 11% visibility of Hong-Ou-Mandel quantum interference verifies the indistinguishability of the heralded single photons after the synchronization. This proof-of-principle demonstration points out the potential significance of the relative multiplexing scheme for large-scale photonic quantum information processing.

OCIS codes: (270.0270) Quantum optics; (270.5585) Quantum information and processing; (060.4230) Multiplexing.

References and links

1. E. Knill, R. Laflamme, and G. J. Milburn, "A scheme for efficient quantum computation with linear optics," Nature **409**(6816), 46–52 (2001).
2. M. Gimeno-Segovia, P. Shadbolt, D. E. Browne, and T. Rudolph, "From three-photon Greenberger-Horne-Zeilinger states to ballistic universal quantum computation," Phys. Rev. Lett. **115**(2), 020502 (2015).
3. T. Rudolph, "Why I am optimistic about the silicon-photonic route to quantum computing," APL Photon. **2**(3), 030901 (2017).
4. M. Tillmann, B. Dakic, R. Heilmann, S. Nolte, A. Szameit, and P. Walther, "Experimental boson sampling," Nat. Photonics **7**, 540–544 (2013).
5. M. A. Broome, A. Fedrizzi, S. Rahimi-Keshari, J. Dove, S. Aaronson, T. C. Ralph, and A. G. White, "Photonic boson sampling in a tunable circuit," Science **339**(6121), 794–798 (2013).
6. J. B. Spring, B. J. Metcalf, P. C. Humphreys, W. S. Kolthammer, X. M. Jin, M. Barbieri, A. Datta, N. Thomas-Peter, N. K. Langford, D. Kundys, J. C. Gates, B. J. Smith, P. G. R. Smith, and I. A. Walmsley, "Boson sampling on a photonic chip," Science **339**(6121), 798–801 (2013).
7. H. Wang, Y. He, Y. Li, Z. Su, B. Li, H. Huang, X. Ding, M. Chen, C. Liu, J. Qin, J. Li, Y. He, C. Schneider, M. Kamp, C. Peng, S. Hofling, C. Lu, and J. Pan, "High-efficiency multiphoton boson sampling," Nat. Photonics **11**, 361–365 (2017).
8. X. L. Wang, L. K. Chen, W. Li, H. L. Huang, C. Liu, C. Chen, Y. H. Luo, Z. E. Su, D. Wu, Z. D. Li, H. Lu, Y. Hu, X. Jiang, C. Z. Peng, L. Li, N. L. Liu, Y. A. Chen, C. Y. Lu, and J. W. Pan, "Experimental ten-photon entanglement," Phys. Rev. Lett. **117**(21), 210502 (2016).
9. X. Ding, Y. He, Z. C. Duan, N. Gregersen, M. C. Chen, S. Unsleber, S. Maier, C. Schneider, M. Kamp, S. Höfling, C. Y. Lu, and J. W. Pan, "On-Demand Single Photons with High Extraction Efficiency and Near-Unity Indistinguishability from a Resonantly Driven Quantum Dot in a Micropillar," Phys. Rev. Lett. **116**(2), 020401 (2016).

#305825 https://doi.org/10.1364/OE.25.026067
Journal © 2017 Received 8 Se- 2017; revised 3 Oct 2017; accepted 4 Oct 2017; published 11 Oct 2017

Optics EXPRESS

10. N. Somaschi, V. Giesz, L. D. Santis, J. C. Loredo, M. P. Almeida, G. Hornecker, S. L. Portalupi, T. Grange, C. Anton, J. Demory, C. Gomez, I. Sagnes, N. D. L. Kimura, A. Lemaitre, A. Auffeves, A. G. White, L. Lanco, and P. Senellart, "Near-optimal single-photon sources in the solid state," Nat. Photonics **10**, 340–345 (2016).
11. J. Spring, P. L. Mennea, B. J. Metcalf, P. C. Humphreys, J. C. Gates, H. L. Rogers, C. Soller, B. J. Smith, W. S. Kolthammer, P. G. R. Smith, and I. A. Walmsley, "A chip-based array of near-identical, pure, heralded single photon sources," Optica **4**(1), 90–96 (2017).
12. C. Reimer, M. Kues, P. Roztocki, B. Wetzel, F. Grazioso, B. E. Little, S. T. Chu, T. Johnston, Y. Bromberg, L. Caspani, D. J. Moss, and R. Morandotti, "Generation of multiphoton entangled quantum states by means of integrated frequency combs," Science **351**(6278), 1176–1180 (2016).
13. A. L. Migdall, D. Branning, and S. Castelletto, "Tailoring single-photon and multiphoton probabilities of a single-photon on-demand source," Phys. Rev. A **66**(5), 053805 (2002).
14. J. Mower and D. Englund, "Efficient generation of single and entangled photons on a silicon photonic integrated chip," Phys. Rev. A **84**(5), 052326 (2011).
15. X. Ma, S. Zotter, J. Kofler, T. Jennewein, and A. Zeilinger, "Experimental generation of single photons via active multiplexing," Phys. Rev. A **83**(4), 043814 (2011).
16. M. J. Collins, C. Xiong, I. H. Rey, T. D. Vo, J. He, S. Shahnia, C. Reardon, T. F. Krauss, M. J. Steel, A. S. Clark, and B. J. Eggleton, "Integrated spatial multiplexing of heralded single-photon sources," Nat. Commun. **4**, 2582 (2013).
17. F. Kaneda, B. G. Christensen, J. J. Wong, H. S. Park, K. T. McCusker, and P. G. Kwiat, "Tim-multiplexed heralded single-photon source," Optica **2**(12), 1010–1013 (2015).
18. G. Mendoza, R. Santagati, J. Munns, E. Hemsley, M. Piekarek, E. M. Lopez, G. D. Marshall, D. Bonneau, M. G. Thompson, and J. L. O'Brien, "Active temporal and spatial multiplexing of photons," Optica **3**(2), 127–132 (2016).
19. C. Xiong, X. Zhang, Z. Liu, M. J. Collins, A. Mahendra, L. G. Helt, M. J. Steel, D. Y. Choi, C. J. Chae, P. H. W. Leong, and B. J. Eggleton, "Active temporal multiplexing of indistinguishable heralded single photons," Nat. Commun. **7**, 10853 (2016).
20. R. J. A. Francis-Jones, R. A. Hoggarth, and P. J. Mosley, "All-fiber multiplexed source of high-purity single photons," Optica **3**(11), 1270–1273 (2016).
21. M. G. Puigibert, G. H. Aguilar, Q. Zhou, M. D. Shaw, V. B. Verma, S. W. Nam, and W. Tittel, "Heralded single photons based on spectral multiplexing and feed-forward control," https://arXiv:1703.02068 (2017).
22. R. A. Hoggarth, R. J. A. Francis-Jones, and P. J. Mosley, "Resource-efficient fibre-integrated temporal multiplexing of heralded single photons," https://arXiv:1706.01828 (2017).
23. M. G. Segovia, H. Cable, G. J. Mendoza, P. Shadbolt, J. W. Silverstone, J. C. Carolan, M. G. Thompson, J. L. O'Brien, and T. G. Rudolph, "Relative multiplexing for minimizing switching in linear-optical quantum computing," New J. Phys. **19**, 063013 (2017).
24. J. Nunn, N. K. Langford, W. S. Kolthammer, T. F. M. Champion, M. R. Sprague, P. S. Michelberger, X. M. Jin, D. G. England, and I. A. Walmsley, "Enhancing multiphoton rates with quantum memories," Phys. Rev. Lett. **110**, 133601 (2013).
25. K. Makino, Y. Hashimoto, J. Yoshikawa, H. Ohdan, T. Toyama, P. van Loock, and A. Furusawa, "Synchronization of optical photons for quantum information processing," Sci. Adv. **2**, e1501772 (2016).
26. F. Kaneda, F. Xu, J. Chapman, and P. G. Kwiat, "Quantum-memory-assisted multi-photon generation for efficient quantum information processing," Optica **4**, 1034–1037 (2017).
27. D. Felinto, C. W. Chou, J. Laurat, E. W. Schomburg, H. D Riedmatten, and H. J. Kimble, "Conditional control of the quantum states of remote atomic memories for quantum networking," Nat. Phys. **2**, 844–848 (2006).
28. J. Cardenas, C. B. Poitras, J. T. Robinson, K. Preston, L. Chen, and M. Lipson, "Low loss etchless silicon photonic waveguides," Opt. Express **17**, 4752–4757 (2009).
29. P. Sibson, J. E. Kennard, S. Stanisic, C. Erven, J. L. O'Brien, and M. G. Thompson, "Integrated silicon photonics for high-speed quantum key distribution," Optica **4**, 172–177 (2017).
30. F. Lenzini, B. Haylock, J. C. Loredo, P. A. Abrahao, N. A. Zakaria, S. Kasture, I. Sagnes, A. Lemaitre, H. P. Phan, D. V. Dao, P. Senellart, M. P. Almeida, A. G. White, and M. Lobino, "Active demultiplexing of single photons from a solid-state source," Laser Photonics Rev. **11**(3), 1600297 (2017).
31. C. K. Hong, Z. Y. Ou, and L. Mandel, "Measurement of subpicosecond time intervals between two photons by interference," Phys. Rev. Lett. **59**(18), 2044–2046 (1987).
32. C. Xiong, X. Zhang, A. Mahendra, J. He, D. Y. Choi, C. J. Chae, D. Marpaung, A. Leinse, R. G. Heideman, M. Hoekman, C. G. H. Roeloffzen, R. M. Oldenbeuving, P. W. L. van Dijk, C. Taddei, P. H. W. Leong, and B. J. Eggleton, "Compact and reconfigurable silicon nitride time-bin entanglement circuit," Optica **2**(8), 724–727 (2015).
33. R. Loudon, *The Quantum Theory of Light*, 3rd ed (Oxford U. Press, 2000).
34. X. Zhang, R. Jiang, B. Bell, D.-Y. Choi, C. J. Chae, and C. Xiong, "Interfering heralded single photon from two separate silicon nanowire pumped at different wavelengths," Technologies **4**, 25 (2016).
35. D. Bonneau, G. J. Mendoza, J. L. O'Brien, and M. G. Thompson, "Effect of loss on multiplexed single-photon sources," New J. Phys. **17**, 043057 (2015).

Optics EXPRESS

1. Introduction

Linear optical quantum computing [1–3] and quantum simulation [4–7] promise an exponential speed up compared to classical information processing for certain tasks. However, to demonstrate quantum supremacy requires increasing the number of synchronized single photons that can be generated simultaneously to ~30-50. This is a formidable challenge, as the probability of *N* single photons (denoted by *N*-photons hereafter) being present simultaneously decreases exponentially with increasing photon number, due to the non-deterministic output of each single photon source [8]. Previous efforts have focused on improving the efficiency of each single photon source with the ultimate goal of achieving deterministic single photon sources. However, neither 'single-emitter' quantum systems [9, 10] nor spontaneous nonlinear optical processes [11, 12] have yet demonstrated a deterministic output. Active temporal or spatial multiplexing has been proposed as a solution [13, 14], and these schemes have been experimentally demonstrated a significant improvement to the single photon generation probability [15–22]. However, experimental efforts to date are still far from the deterministic regime, due to technical challenges such as the loss incurred in delay lines and active switches. Recent work [23], M. G. Segovia et al. has proposed a relative multiplexing scheme that considers *N* single photon sources as one entity and actively synchronizes heralded single photons, as shown in Fig. 1(a). Theoretical analysis indicates a significantly enhancement in *N*-photons generation probability without increasing the complexity compared to pre-existing multiplexing schemes.

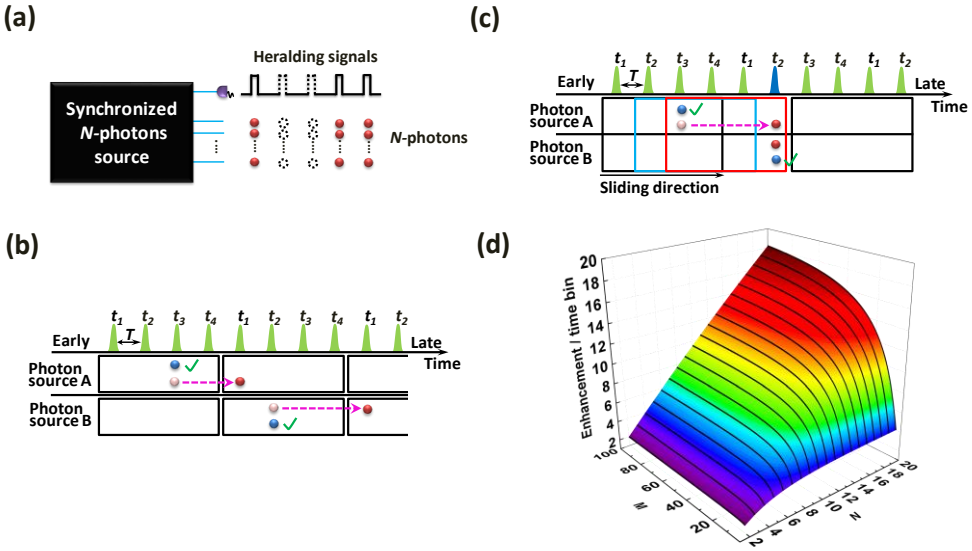

Fig. 1. (a) Schematic of a synchronized *N*-photons source. Heralding signals indicate the existence of an *N*-photons state. The dashed lines and circles represent no heralding signals and *N*-photons at that time-bin, respectively. (b) The principle of the STM scheme. Laser pulses (green) define the time-bins with a period of *T*. The rectangles represent the time windows, each containing 4 time-bins. The blue circles are the heralding photons. The light red and red circles are the heralded photons before and after shifting, respectively. (c) The principle of the RTM scheme. The rectangles of different colors indicate the time windows being slid by *T* per step. The blue pulse indicates the time-bin of the output heralded photon pair. (d) Enhancement between RTM and STM. *M* is the number of time-bins per time window and *N* is the number of photon sources included in the scheme.

In this paper, we systematically analyze the benefits of a relative temporal multiplexing (RTM) scheme and report on the experimental implementation using two nonlinear single photon sources. Experimental results show that the probability of generating heralded photon pairs is enhanced by an additional 90%, compared to the standard temporal multiplexing

Optics EXPRESS

(STM) scheme. Furthermore, the additional enhancement increases with the number of photons and temporal modes to be multiplexed. Hong-Ou-Mandel quantum interference between the two heralded photons shows a visibility of 88 ± 11% after subtracting noise counts, indicating that the multiplexed photons are highly indistinguishable. The experimental results show that RTM is a scalable and efficient scheme for the *N*-photons generation, which will boost the potential applications of large-scale photonic quantum information processing.

RTM is conceptually similar to synchronizing heralded single photons using a quantum memory [24]. Previous works have used quantum memories based on low loss cavities [25, 26] or cold atomic ensembles [27] to significantly enhance the count rate of synchronized photons. The RTM scheme is mainly distinguished by its potential scalability to many sources. Here, we make use of fiber-based switches and delay lines, which in future could be replaced by integrated photonic components [28, 29] to allow *N*-photon state generation on an integration platform. The number of temporal modes which can be multiplexed grows exponentially with the number of switches and delay lines, so, provided low loss components are available, relatively few switches are required to create a large enhancement.

2. Principle and experimental setup

To clearly illustrate the advantages of RTM over STM, we first explain the principle of the STM scheme. In this scheme, *N* heralded single photon sources are pumped by synchronized laser pulses separated by a period of *T*, which are grouped into time windows containing *M* laser pulses or time-bins. Figure 1(b) illustrates the principle of the scheme for the number of sources $N = 2$ (photon sources A and B) and time bins $M = 4$ (time-bins are labeled as t_1 to t_4). Heralding photons (blue) are detected and their time-bin information is used to delay the heralded photons (red) to t_1 by actively configuring a delay line. In the STM scheme, a heralded *N*-photons state is generated whenever each single photon sources emit photons within the same time window. The rate per time-bin can be expressed as

$$P_{\mathrm{STM/time\ bin}} = M^{N-1}\mu^{N}. \tag{1}$$

where μ is the probability of one source generating a heralded single photon in one time-bin. Equation (1) is an approximate form which holds when the probability of each source emitting per time window remains low, $M\mu \ll 1$.

Figure 1(c) depicts the principle of the RTM scheme [23]. The time window (rectangle) is translated to begin at each time-bin. If all *N*-heralding photons are detected within one time window, the heralded photons are delayed to align with the latest one; otherwise they are abandoned. The heralded photons are equally likely to appear in any time-bin and the sliding window includes additional opportunities to generate *N*-photons, which would be otherwise ignored in the STM scheme where heralded photons belong to different windows. Moreover, less demand is placed on the speed of the switches, as they are only triggered by the detection of *N*-heralding photons within one time window, rather than for every single heralding photon. The rate of *N*-photons state per time-bin, again assuming $M\mu \ll 1$, is expressed as

$$P_{\mathrm{RTM1/time\ bin}} = (M^{N} - (M-1)^{N})\mu^{N}. \tag{2}$$

Here, RMT1 represents the first strategy for RTM in this work. Another strategy, RTM2, will be explained in the following section. The additional enhancement between RTM1 and STM is

$$P_{\mathrm{RTM1/time\ bin}} / P_{\mathrm{STM/time\ bin}} = (M^{N} - (M-1)^{N}) / M^{N-1}, \tag{3}$$

and a plot of Eq. (3) for different values of *M* and *N* is shown in Fig. 1(d). The maximum value of additional enhancement increases with *N*, so this scheme could be highly beneficial

Optics EXPRESS

in future *N*-photon interference experiments. The derivation of each equation is described in detail in Appendix I.

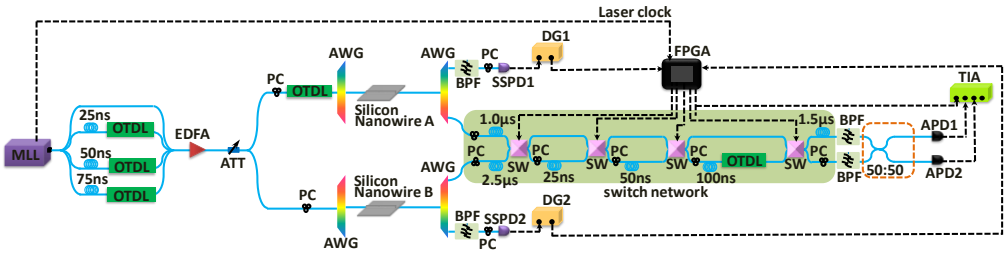

Fig. 2. Experimental setup. MLL: mode-locked laser, PC: polarization controller, OTDL: optical tunable delay line, EDFA: erbium-doped fiber amplifier. ATT: attenuator, AWG: array waveguide grating, BPF: band pass filter, DG: delay generator, SSPD: superconducting single photon detector, APD: avalanche photon diode, TIA: time interval analyzer. SW: switch, Solid and dashed lines represent optical fibers and electronic cables, respectively.

Figure 2 illustrates the experimental setup. 10 ps optical pulses (green pulses) are emitted from a 10 MHz mode-locked laser (MLL) at a central wavelength of 1555.7 nm. The period is reduced from 100 ns to 25 ns by splitting the pulse into four paths; with separate delay fibers and optical tunable delay lines (OTDL) between recombining the paths at a 1-to-4 directional coupler. The erbium doped fiber amplifier (EDFA) amplifies the 40 MHz pump pulses and the average pump power applied on two nominally identical silicon nanowires are controlled by the attenuator (ATT) before the arrayed waveguide gratings (AWG). Two nominally identical silicon nanowires (3 mm long) are simultaneously pumped to generate correlated photon pairs in random time-bins via spontaneous four-wave mixing (SFWM). The insertion loss of each silicon nanowire is around 6 dB. Two Gaussian shaped AWGs with 0.4 nm bandwidth and 3 dB insertion loss are used to spatially separate photon pairs generated at 1550.9 nm and 1560.5 nm and to block the pump laser. The pump photons are further suppressed by a band pass filter (BPF) with 0.5 nm bandwidth and 2 dB insertion loss. A polarization controller with 1 dB insertion loss is connected before SSPD to maximize the detection efficiency. After being detected by SSPD with around 20% detection efficiency, the detection signals are shifted by DG (DG645 Stanford Research System) and their time-bin information is recognized by the FPGA. If heralding photons from both sources appear within one time window, the FPGA actively controls the switch network to synchronize these two heralded photons. Meanwhile, it sends a heralding signal at the time bin of the heralded photon pair to the time interval analyzer (TIA). The switch network contains four ceramic switches and it is shared by the two sources, using additional fibers before the first switch to introduce 1 μs and 2.5 μs delay for source A and B, respectively. Each ceramic switch has 1-2 dB insertion loss and the additional delay fiber introduces 2-3 dB loss, mainly due to connector losses, since it is built from separate fibers. These buffer fibers guarantee the heralded photons from two sources are well separated when they pass through the switches. Thus, the switches can be configured independently for heralded photons from different sources. A 1.5 μs delay (2-3 dB loss) after the network compensates the difference in time delay between the two heralded channels. The OTDL in the switch network adds 2 dB loss into the heralded channels. The 50:50 coupler is only used for a Hong-Ou-Mandel (HOM) quantum interference measurement. Heralded photons are finally detected by two avalanche photon diodes (APD: ID210, Id-Quantique). The detection efficiency of each detector is set to 25%. The heralding signals from the FPGA and the detection of the heralded photon pair from avalanche photodiode (APDs) are collected by the TIA as the start and stop signal of 4-fold coincidences, respectively. The overall collection efficiencies of heralding and heralded channel are around 17 dB and 28 dB respectively. Nevertheless, the collection efficiency can be significantly improved with low loss components and high efficiency detectors. Using

Optics EXPRESS

separate switch networks for each source would also allow the additional delay fibers to be removed.

3. Results and discussions

To experimentally demonstrate the additional enhancement of RTM, we implement a 4-fold coincidence measurement and compare the 4-fold counts between the STM and RTM1 schemes. Figure 3 summarizes the measurement results in each scheme. With the same average pump power (0.52 mW), the 4-fold coincidence counts of STM and RTM1 in one hour are 19 and 37, respectively, shown as pink bars in Fig. 3. After subtracting uncorrelated noise, the net 4-fold coincidence counts of STM and RTM1 are 15 and 29, respectively. The uncorrelated noise counts in RTM1 are higher than STM, because the heralded photon pairs are actively synchronized at any time-bin in RTM1 rather than a fixed time bin (t_1) in STM so the APD must be triggered at 40 MHz rather than at 10 MHz. The enhancement ratio between STM and RTM1 is 1.95 ± 0.5, which is higher than, but within an error-bar of, the expected value of 1.75 calculated from Eq. (3). The large error margin results from the Poissonian statistics of the low count. In the future, the count rate can be improved by using high efficiency single photon detectors and low loss components [30]. Meanwhile, we also monitor the heralding signal rate during the measurement, shown as blue bars in Fig. 3. The ratio between these two schemes, 1.86 ± 0.05, further confirms the additional enhancement in RTM, as the heralding signal rate is proportional to the generation rate of heralded photon pairs.

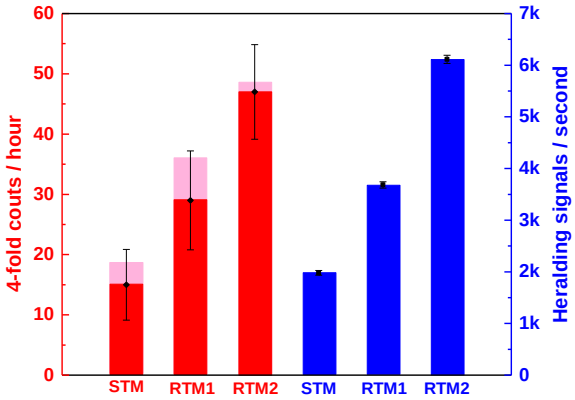

Fig. 3. The pink and the red bars represent the raw and net 4-fold coincidence counts in one hour, respectively. The blue bars represent the average heralding signal rate during the same measurement time. The error is based on the Poissonian statistics of the count rates.

The indistinguishability of heralded photons is a crucial requirement for photonic quantum interference. It requires two heralded photons be synchronized to within a coherence length after the switch network, regardless of which time-bin they originate from. This is usually verified by Hong-Ou-Mandel (HOM) quantum interference [31]. The delay lines in the switch network are manually cut, making it challenging to control them with picosecond accuracy. In STM, the tiny deviation in these delay lines can be compensated by adjusting the timing of the pump pulses using the OTDLs before the sources, avoiding the additional loss of tunable delay lines in the single photon channels [19]. However, the strategy of unevenly spaced pump pulses cannot result in perfectly synchronized photons in RTM since heralded photons can be shifted to any time bin instead of a fixed one. This problem could be solved in integrated photonic circuits [32], where waveguides can be fabricated to provide precise delays. Here, we adopt a hybrid strategy of RTM that combines STM and RTM1 to verify the indistinguishability. In this hybrid strategy, heralded photons are first precisely shifted to the next t_1 time-bin, as in STM. Then RTM is applied between adjacent t_1 time-bins using the 100

Optics EXPRESS

ns delay in the switch network, as shown in Fig. 4(a). The 100 ns delay in the switch network contains an OTDL so that the shifted photons remain indistinguishable, as shown in Fig. 2. In the hybrid strategy, the maximum time window has been extended from 75 ns to 175 ns so that additional heralded photon pairs can be synchronized compared to RTM1 and STM. The probability of generating heralded photon pairs per time bin, assuming $M\mu \ll 1$, is expressed as:

$$P_{\mathrm{RTM2/time\ bin}} = M^{N-1}\mu^{N}(2^{N}-1). \tag{4}$$

Here, RTM2 represents the hybrid strategy of the RTM. The additional enhancement between RTM2 and STM can be expressed as:

$$P_{\mathrm{RTM2/time\ bin}} / P_{\mathrm{STM/time\ bin}} = M^{N-1}(2^{N}-1). \tag{5}$$

Equations (4) and (5) are described in detail in Appendix I. The net (raw) 4-fold coincidence counts in one hour is 47 (48) and the heralding signal rate is around 6 kHz, shown as RTM2 in Fig. 3. The three-fold enhancement compared to STM is in good agreement with Eq. (5).

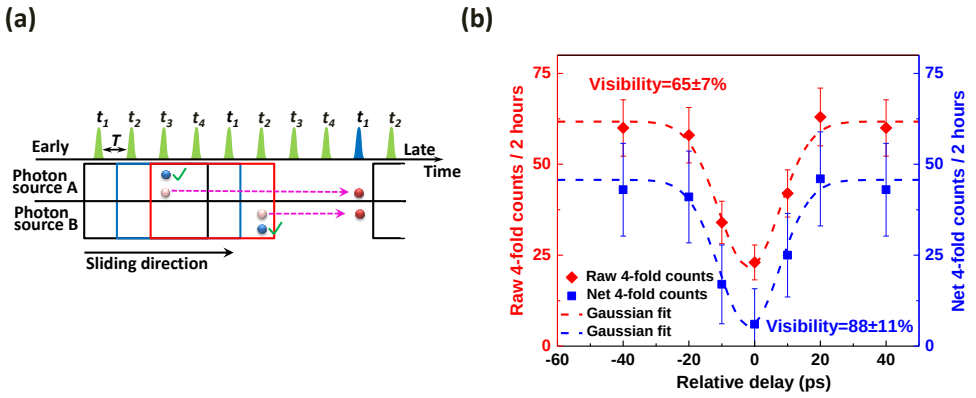

Fig. 4. (a) The principle of the RTM2. (b) Hong-Ou-Mandel quantum interference results. The red diamonds are the 4-fold coincidence counts with noise, represented by the raw 4-fold counts. The blue rectangles are the 4-fold coincidence counts after subtracting noise counts, represented by the net 4-fold counts. The dash line is Gaussian fit. Poisson error bar is used for plot.

After matching the polarizations and precisely synchronizing the heralded photons [19], we implement a HOM quantum interference experiment. When the relative delay (t_R) between two heralded single photons is larger than the coherence time (10 ps), the 4-fold coincidence count (red diamonds) measured in two hours is around 60. This value reduces to 23 when t_R is negligible. t_R is precisely controlled by the OTDL without changing the polarization. In Fig. 4(b), a 65 ± 7% interference visibility is estimated by a Gaussian fit to the 4-fold coincidence measurement (red). Here, the visibility is relatively low due to the high multi-photon emission probability from each source. It is necessary to use high power in our experiment to boost the counts rate because of the high losses. A lower pump power can be applied to reduce multi-photon noise if low loss components become available or even photon number resolving detectors can be used to discard multi-photons. We experimentally measured the multi-photon noise from each source with the method explained in [19]. After subtracting this background, the HOM visibility is 88 ± 11%, indicated by the Gaussian fit. This demonstrates that the heralded single photons are highly indistinguishable from each other, as it is far above the classical threshold of 50% [33] and comparable to the HOM visibility when multiplexing is not used [34].

Optics EXPRESS

4. Conclusions

In this work, we have experimentally demonstrated a relative temporal multiplexing scheme and systematically analyzed its benefits. The 4-fold coincidence measurement and the quantum interference demonstrate that the RTM scheme can generate indistinguishable single photons with additional enhancement over STM and the theoretical analysis indicates the additional enhancement will increase with the number of single photon sources. The four-photon count rate is low due to the high collection, filtering and detection losses of the single photon sources, but this proof-of-principle demonstration clearly shows the benefit of RTM over STM. The overall enhancement of RTM is also intrinsically determined by the number of switches and the loss of each switch [19, 35]. RTM greatly relaxes the speed requirement of the switches, which are only triggered for heralded *N*-photons instead of for each heralded single photon. This feature is a crucial advantage when μ is increased and large numbers of temporal modes are included in the time window, since fast, low-loss and low-noise switches are unavailable. Besides the additional enhancement and the relaxed switching requirement illustrated in the RTM scheme, the heralding signal can be used to further synchronize *N*-photon states generated from RTM. Future improvements, including the use of high-efficiency detectors or even photon-number-resolving detectors and the development of low-loss filters, are possible to much more efficiently produce *N*-photon states for potential applications in large-scale photonic quantum information processing.

Appendix I: Theoretical equation of each scheme and the enhancement

In the STM scheme, each single photon source implements temporal multiplexing independently, relocating heralded photons from many temporal modes to a fixed temporal mode, such as t_1. We assume that *N* single photon sources implement the STM scheme and each time window is formed by *M* laser pulses with a period of *T*. The probability of generating single photons from one source per time window can be strictly expressed as

$$P_{\text{source/window}} = 1-(1-\mu)^M \tag{6}$$

where μ is the probability of one source generating single heralded photon per pump pulse or time bin. To avoid multi-photon noise, μ is limited to a trivial value in the experimental demonstrations, $\mu \ll 1$. Thereby, Eq. (6) can be expressed as

$$P_{\text{source/window}} = M\mu. \tag{7}$$

Base on Eq. (7), the probability of generating *N* single photons (denoted by *N*-photons hereafter) from *N* sources per time window can be expressed as

$$P_{\text{STM/window}} = M^N \mu^N, \tag{8}$$

with a further assumption, $M\mu \ll 1$. Since each time window contains *M* time-bins, the probability of generating *N*-photons per time bin can be expressed as

$$P_{\text{STM/time bin}} = M^N \mu^N / M = M^{N-1}\mu^N. \tag{9}$$

Multiplying this probability by the repetition rate of the laser gives the generation rate of *N*-photons.

In the RTM scheme, *N* single photon sources implement temporal multiplexing as one unit and each heralded photon is shifted to align with the latest one when each photon source emits a heralding photon within the same time window, otherwise these heralded photons are abandoned. The time window (rectangle) is translated to begin at each time-bin. With the same assumption, $M\mu \ll 1$, the probability of generating *N*-photons within one time window

Optics EXPRESS

in RTM is given by Eq. (8). To correctly find the probability per time bin, we have to exclude the events of *N*-photons where no single photon originates from the latest time-bin of the time window, since these events already have been synchronized by an earlier window. The events to exclude are the ones where *N*-photons occur in the first *M-1* time-bins of a time window, which occur with the probability of $(M-1)^N \mu^N$. This probability holds in the limit of small $M\mu$ and this part should be subtracted from the total probability per time window to give the probability of generating *N*-photons per time bin in RTM

$$P_{\mathrm{RTM1/time\ bin}} = M^N \mu^N - (M-1)^N \mu^N. \tag{10}$$

Here, RTM1 represents the first of two strategies for RTM in this work. The enhancement ratio between RTM1 and STM can be expressed as

$$P_{\mathrm{RTM1/time\ bin}} / P_{\mathrm{STM/time\ bin}} = (M^N - (M-1)^N) / M^{N-1}. \tag{11}$$

In this work, we also adopt another hybrid strategy of RTM to verify indistinguishability of heralded single photons. Instead of *N*-photons state appearing at a random time bin, we synchronize every heralded photon to one fixed temporal mode, t_1 and also apply the 100 ns delay on the heralded single photon if the required delay is larger than 4 time bins. In this case, the maximum switchable delay has been extended from 75 ns to 175 ns. It enhances the generation probability of *N*-photons state to three-fold compared with the STM scheme. Because it contains three combinations: the heralded photons appear within the same time window, a heralded photon from source A appears in the time window following one from source B, or a heralded photon from source B appears in the time window following one from source A. In a more general scenario with *N* photon sources, the probability of generating *N*-photons per multiplexing window is approximately expressed as

$$P_{\mathrm{RTM2/window}} = M^N \mu^N (2^N - 1). \tag{12}$$

Here, RTM2 represents the second hybrid strategy for RTM. Equation (12) also holds the same assumption, $M\mu \ll 1$. The probability per time bin can be expressed as

$$P_{\mathrm{RTM2/time\ bin}} = [M^N \mu^N (2^N - 1)] / M = M^{N-1} \mu^N (2^N - 1). \tag{13}$$

The additional enhancement between RTM2 and STM is expressed as

$$P_{\mathrm{RTM2/time\ bin}} / P_{\mathrm{STM/time\ bin}} = [M^{N-1} \mu^N (2^N - 1)] / (M^{N-1} \mu^N) = (2^N - 1). \tag{14}$$

Funding

Centre of Excellence (CUDOS, CE110001018); Laureate Fellowship (FL120100029); Discovery Early Career Researcher Award (DE120100226); Future Fellowship (FT110100853); Huawei Technology Inc.